# Personalized anti-cancer drug combination prediction by an Integrated Multi-level Network

Running title: Network-based prediction of anti-cancer drug combination

**Fangyoumin Feng[1,2,3], Zhengtao Zhang[2,4], Guohui Ding[1,5], Lijian Hui[2,4,6,7], Yixue Li[1,2,3,8*], Hong Li[1*]**

1. CAS Key Laboratory of Computational Biology, CAS-MPG Partner Institute for Computational Biology, Shanghai Institute of Nutrition and Health, Shanghai Institutes for Biological Sciences, Chinese Academy of Sciences, Shanghai 200031, China
2. University of the Chinese Academy of Sciences, Beijing 100049, China
3. School of Life Science and Technology, ShanghaiTech University, Shanghai 201210, China
4. State Key Laboratory of Cell Biology, CAS Center for Excellence in Molecular Cell Science, Shanghai Institute of Biochemistry and Cell Biology, Chinese Academy of Sciences, Shanghai 200031, China
5. Anhui Engineering Laboratory for Big Data of Precision Medicine, Anhui, 234000, China
6. Institute for Stem Cell and Regeneration, Chinese Academy of Sciences, Beijing 100101, China.
7. Bio-Research Innovation Center, Shanghai Institute of Biochemistry and Cell Biology, Suzhou 215121, Jiangsu Province, China
8. Collaborative Innovation Center of Genetics and Development, Fudan University, Shanghai 200433, China

*Corresponding to Hong Li (lihong01@sibs.ac.cn) or Yixue Li (yxli@sibs.ac.cn)

# Abstract

Anti-cancer drug combination is an effective solution to improve treatment efficacy and overcome resistance. Here we propose a network-based method (DComboNet) to prioritize the candidate drug combinations. The level one model is to predict generalized anti-cancer drug combination effectiveness and level two model is to predict personalized drug combinations. By integrating drugs, genes, pathways and their associations, DComboNet achieves better performance than previous methods, with high AUC value of around 0.8. The level two model performs better than level one model by introducing cancer sample specific transcriptome data into network construction. DComboNet is further applied on finding combinable drugs for sorafenib in

hepatocellular cancer, and the results are verified with literatures and cell line experiments. More importantly, three potential mechanism modes of combinations were inferred based on network analysis. In summary, DComboNet is valuable for prioritizing drug combination and the network model may facilitate the understanding of the combination mechanisms.

*Keyword*

Cancer, Drug Combination, Multi-level Heterogeneous Network, Drug Induced Transcriptomic Changes

# Background

Cancer is the leading life-threatening disease across the world with more than eighteen million new diagnosed cancer cases and 9.6 million death in 2018 [1]. Due to the genetic and phenotypic heterogeneity of cancer, conventional anti-cancer monotherapies could not reach the expectation of clinical outcome. Unavoidable resistance and side effects induced by some monotherapies require effort on exploring more effective treatment strategies. Therefore, combining anti-cancer medicines has become a feasible alternative because of their advantages on sensitizing cancer response, modulating multiple biological progresses or pathways and reducing side effects[2]. Till 2015, only 49 anti-cancer combinatorial chemotherapies have been approved by FDA [3]. To discover more drug combinations, several high-throughput drug combination screening on cancer cell lines have been established which allow hundreds of drug

pairs being tested in short time [4]. However, experimental screening all anti-cancer drug pairs exhaustively is impractical. Thus, in-silico discovery of potential drug combinations is considered as a reasonable way.

Two major strategies are considered for constructing more precise prediction models, that is to predict whether drugs can combine to achieve synergism and if the combinations can combine in a certain disease context. To address the former questions, methods like Zhao's integrated drug-drug similarities including drug indication, drug ATC code, drug target proteins and drug side effects to predict effective drug combinations[5]. With the accumulation of cancer sample/cell lines transcriptome data and the understanding of molecular mechanism between drug and cancer, drug combination prediction in the context of cancer sample has gradually become the main direction. Databases like CCLE and LINCS released drug treated cancer cell line transcriptome data offer a solid base to support the construction of a cancer-specific dynamic network which reflect the real drug function [6-8]. Dialogue for Reverse Engineering Assessments and Methods consortium (DREAM) launched a worldwide open challenge in 2014 for drug synergy/combination prediction aimed at developing prediction models based on the integration of multilevel data [9]. Among the 31 submitted models, DIGRE, the top one algorithm, predict drug synergy based on modelling drug combination induced transcriptome changes from monotherapy perturbations[10]. SynGen predict combinable drug pairs which work complementary towards master regulators who induce cell death or inhibiting cell status activation [9]. Following the challenge, Cao et al, proposed a well performed model compared with other methods based on semi-supervised learning called RACS[11]. It integrated seven features from drug targeting networks and two filtering parameters from transcriptomic profiles

and predicted potential drug combination based on the similarities to positive dataset. Though the features in RACS and other models were more focusing on local similarity between drug targets or the function of targets, the integration of multi-level drug related information and the combination of targeting network and drug treatment transcriptome profile provide a new notion of building a dynamic disease network interpreted by drug treatment. With the accumulation of high-throughput drug screening data, several supervised models have been built based on large high-throughput drug synergy screen dataset, like 39 drugs for 38 cancer cell lines provided by O'Neil [12] and 710 drug combinations across 85 cancer cell lines in drug synergy prediction DREAM challenge [13]. Algorithms like DMIS, NAD and Y Guan, performed in top three position in DREAM challenge, predict drug synergism on cell lines via multi-dimensional feature extraction and machine learning methods[13]. These algorithms showed good performance on the data set provided by DREAM[13]. Later on, deep learning model Deepsynergy used similar strategy achieve good performance[14]. However, these supervised learning algorithms tend to have high dependence on a large number of cell line experimental data to achieve good predictions on the corresponding cell lines. Furthermore, the algorithms are usually difficult to apply on other cell lines than the modelling set. When tested on the O'Neil data set, the performance of Y Guan, DMIS, NAD are all dropped[13]. Although performed well on cross-validation on modelling dataset, Deepsynergy did not verify in external dataset[14].

The complexity of drug mechanism on real cancer context is still a main obstacle in combination prediction. Constructing a heterogeneous network is an applicable solution for integrating multilevel information and modeling different biological systems[15, 16]. Han's

method mapped drug on gene expression profile weighted PPI network via drug-target associations to predict drug-drug interactions [17]. WNS method evaluated drug synergy in pathway-pathway interaction network [18]. DrugComboRanker discovered potential drug combination by identifying drug-drug associations in target networks[19]. Barabasi's synergy prediction is based on measuring the distance between drug modules and disease modules discovered from the gene network between drug targets and disease related genes[20]. In addition to use in predicting synergistic drug combinations, network-based approaches may help infer potential mechanism between combinable drug pairs via the construction of biological network[15]. However, these network-based methods based mainly on drug and their known direct target genes, even with the integration of pre-treatment transcriptome data, they did not show enough power to predict sample-specific drug combinations.

Assuming pharmacologically similar and functionally related drugs tend to combine together, we proposed a computational method called DComboNet to predict the anti-cancer drug combination. The DComboNet level one model constructs a generalized heterogeneous network integrating drug-drug, drug-gene, drug-pathway, gene-gene and pathway-pathway associations. Drugs that can be combined with the drug seed are predicted according to their global similarity in the network. The level two model constructs a cancer sample specific network to predict personalized drug combination. DComboNet was evaluated using cross validation, independent test and experimental validation. DComboNet outperformed the previous methods. Additionally, DComboNet provides clues for the potential mechanisms of drug combinations.

# Results

## Characteristics of know anti-cancer drug combinations

We collected 218 known anti-cancer drug combinations that involved in 157 drugs. There were three types of drugs: 67 standard chemotherapy (C), 57 targeted cancer therapy (T) and 33 other kind of drugs (O) (**Fig. 1a)**. The effects and anti-tumor mechanisms of these three types drugs are distinctive. Standard chemotherapy acts on both normal and cancerous cells via their cytotoxic function; targeted cancer therapies are deliberately chosen or designed to interact with their specific target or targets with a cytostatic mechanism; other drugs may help control cancer related complications or alleviate on side effects caused by anti-cancer medicine. The combinations within and between three types can all be seen in known anti-cancer drug combination (**Fig. 1b**).

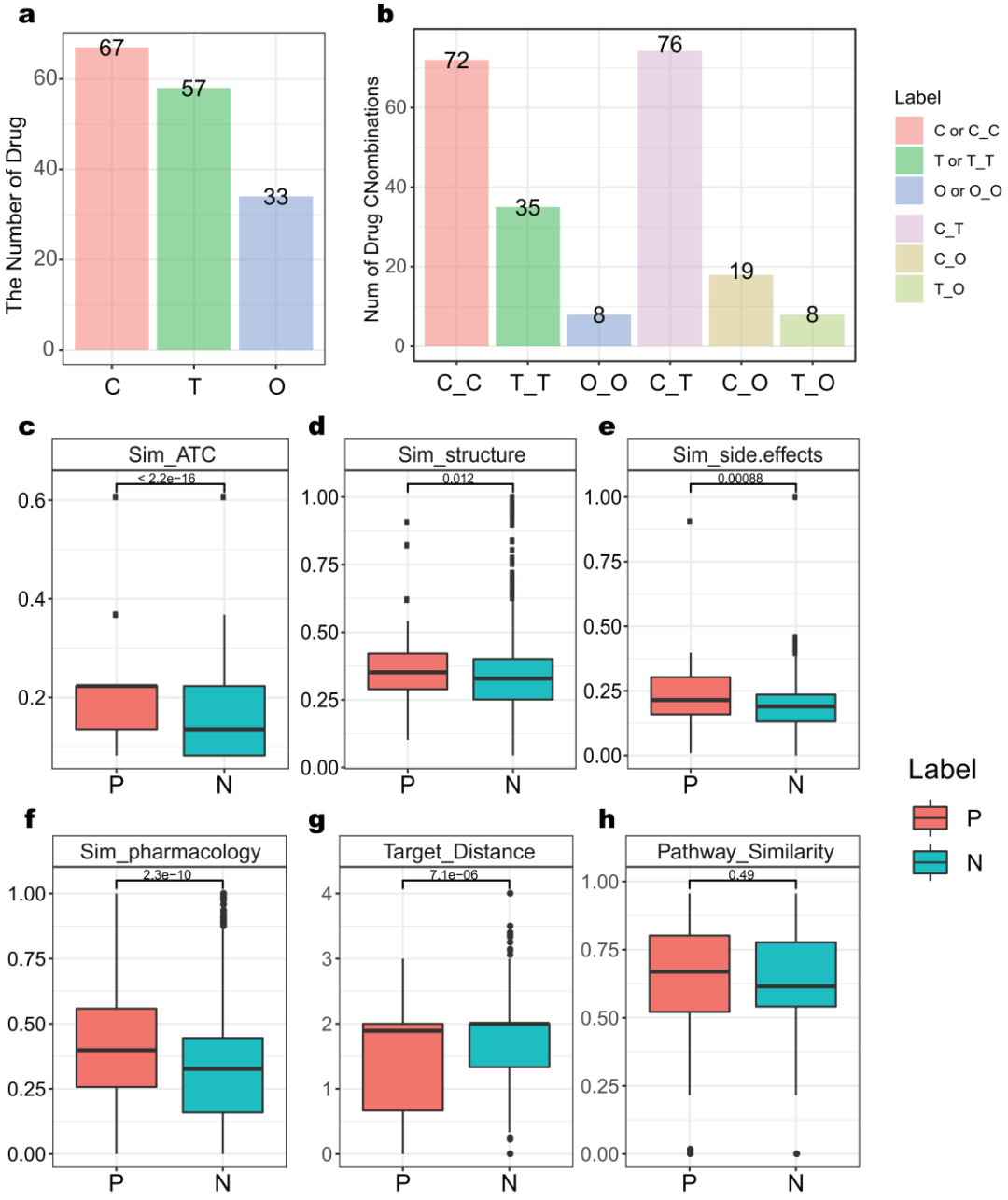


**Figure 1**. Features of known anti-cancer drug combinations. **a** The distribution of drug types. C, T and O are standard chemotherapy, targeted cancer therapy and other cancer-related drugs, respectively. **b** The distribution of drug combinations by drug types. **c-e** Comparison of ATC code similarity, chemical structural similarity and side-effect similarity between known drug combinations (P) and unlabeled drug pairs (N); **f-h** Comparison of the integrated pharmacological similarity, target distance and pathway similarity between known anti-cancer drug combinations (P) and unlabeled drug pairs (N).

The mechanisms of drug combinations can be partially explained by pharmacological similarity, topological associations of drug targeted genes and functional pathways[5, 11, 18]. To understand the contribution of these features to anti-cancer drug combinations, we generated 9017 unlabeled

drug pairs by randomly pairing the drugs in the positive dataset and then compared unlabeled pairs with known combinations. The ATC code, chemical structure fingerprints and side effects were used to calculated the similarity between drug pairs respectively (**Supplementary methods**), and then combined into an integrated pharmacological similarity. All the single and integrated pharmacological similarity were higher in known combinations than in unlabeled pairs (**Fig.1c-f**). Target distance was the average distance between two target gene sets on the background gene-gene interaction network. Drugs in known combinations had shorter target distance than in unlabeled pairs (**Fig. 1g**). Pathway similarity between drugs was implemented via computing the average shortest distance between pathways, and if drugs co-regulate same pathway, using the shortest distance between their targeted genes to represent their pathway similarity. (**Supplementary methods**). The pathway similarity of drugs in known combinations is also higher than randomized pairs, though not significant (**Fig1h**). Therefore, we thought integrating both drug pharmacological and functional associations may help predict combinable drug pairs and reveal the potential mechanisms.

## Workflow of cancer drug combination network (DComboNet)

The concept of DComboNet is to abstract pharmacological and functional relationships between drugs into a heterogeneous cancer drug combination network **(Fig 2a**). DComboNet consists of five subnetworks: drug-drug association network ($N_{DD}$), drug-gene association network ($N_{DG}$), gene-gene association network ($N_{GG}$), drug-pathway association network ($N_{DP}$) and pathway-pathway association network ($N_{PP}$).

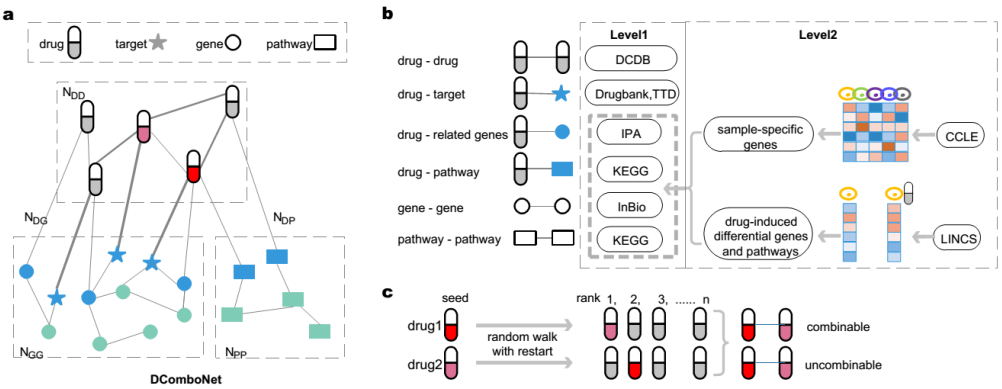


**Figure 2**. Workflow of drug combination prediction model (DComboNet). **a** Construction of heterogeneous cancer drug combination network (DComboNet). The network contains five sub-networks, $N_{DD}$ indicates drug-drug association network, $N_{DG}$ indicates drug-gene association network, $N_{GG}$ indicates gene-gene association network, $N_{DP}$ indicates drug-pathway association network and $N_{PP}$ indicates pathway-pathway association network. **b** Source and methods for generating network edges. Level one indicates the generalized model and level two indicates cancer sample specific model. **c** Method of ranking drug pairs.

DComboNet contains two levels of models (**Fig. 2b**). Level one is a general model that predict the potential drug combinations. It was established without considering individual heterogeneity. Edges were generated from multiple databases and the weights of edges were assigned based on the edge types (seeing **Methods**). Level one model may be not precise enough for specific cancer type or individual sample. Introducing transcriptome data into drug combination prediction can enhance the precision of the prediction for certain cancer type [10]. Therefore, level two model utilized transcriptome data to reconstruct networks and predict drug combinations for a specific cancer sample. Sample specific expressed genes were obtained by comparing the expression profile of this sample with other cancer samples. Drug induced differentially expressed genes and pathways were obtained by comparing the expression profiles before and after drug treatment.

After network construction, Random Walk with Restart method was applied to capture the global proximity between the given drug seed and candidate drugs in the network. For a drug pair, drug1 and drug2, take each of them as seed to calculate the global proximity between drug1

and drug2, respectively. Then a two-threshold strategy was used to integrate two ranks and classify the drug pair into combinable, uncombinable and intermediate (**Supplementary methods**).

## Performance of level one model

Leave-one-combination-out cross validation (LOCOCV) was used to evaluate the performance of level one model. Firstly, we compared the prediction performance of using drug-drug network alone and using the integration of multiple different networks. DComboNet integrated five subnetworks and obtained the best performance (**Fig.s1c**). The AUC of DComboNet is 0.797 and the true positive rate (TPR) is 63.24%. Secondly, we compared the prediction results of different drug types (**Fig. 3 a-b**). Standard Chemotherapy combinations (C-C) performed well with AUC equals to 0.816. All 68 real drug combinations within this category were ranked in top 50%, of which 51 known combinations were predicted to as combinable. Targeted therapy drug combinations (T-T) also achieved high accuracy with 17 out of 23 known combinations were predicted correctly (TPR = 76%). Due to the lack of pharmacological and functional associations between standard chemotherapy and targeted therapy, the accuracy of C-T combinations is slightly less powerful (TPR = 53.52%). Lastly, we compared DComboNet with a previous published algorithm, RACS preliminary model, which also predict without using transcriptome data [11]. DComboNet outperformance RACS which has AUC equal of 0.548 and true positive rate 46.0% (**Fig. 3c**).

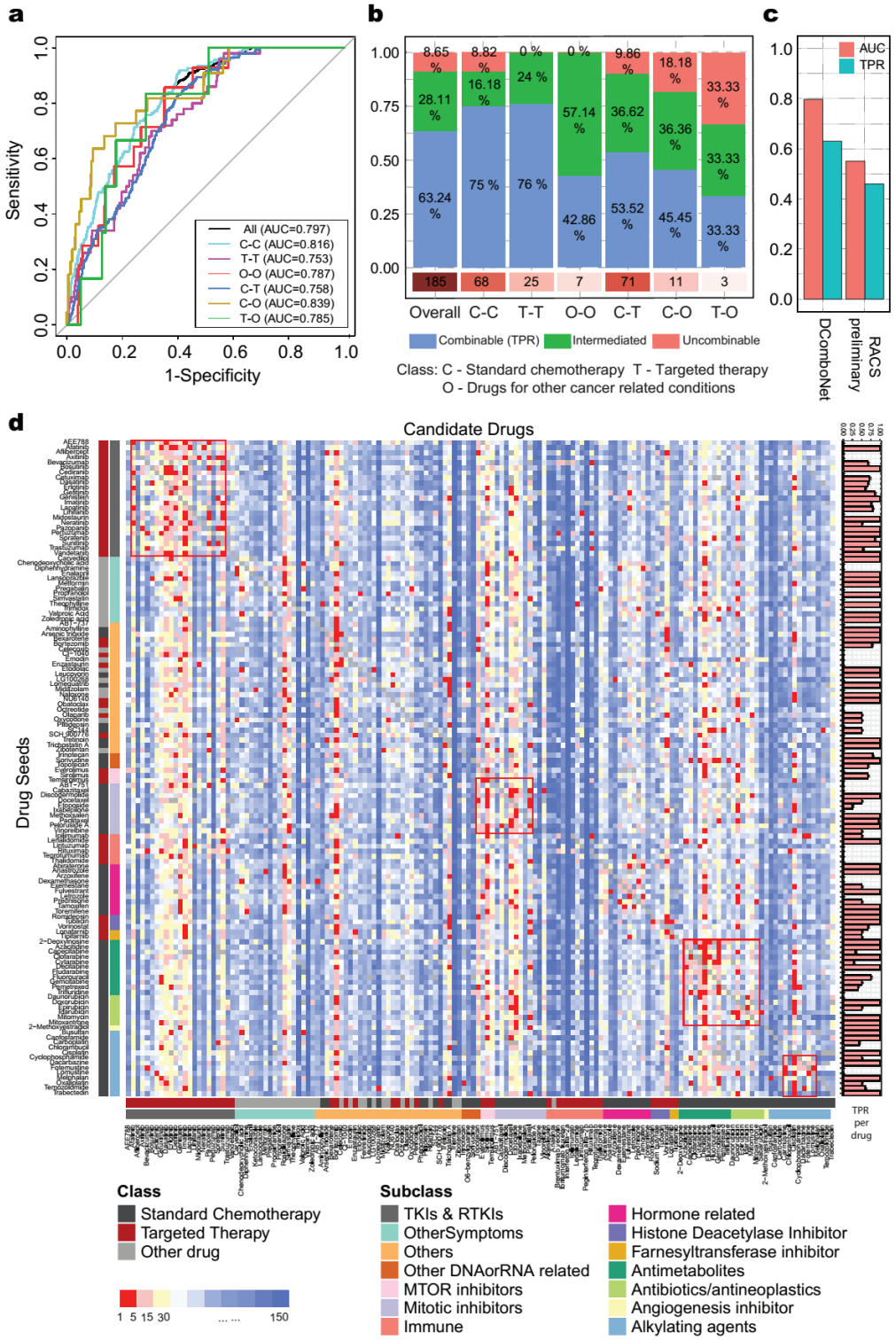


**Figure 3**. Performance of the level one model. **a** ROC plots and AUC values based on different types of drug combinations. **b** The percentage of predicted as combinable, uncombinable and intermediate in known drug combinations with respect to different drug combination types. **c** Comparison of performance between DComboNet and RACS preliminary. **d** The result of Level one model DComboNet. Heatmap was sorted in two directions according to drug subclasses (**Table s1**). Each row represents a drug seed. Color in the plot shows the rank of similarity between drug seed and other drugs. The bar plot on the right shows the successfully predicted drug pairs

in known combinations (TPR for each drug seed).

Furthermore, we used DComboNet to predict the combination potentially of all drug pairs. (**Fig. 3d**). In order to better analyze the prediction result, we further categorize drugs into 12 subtypes based on their mechanism of action. We found drugs within the same subtype are more likely to be recommended as combinable drugs because of their relevant functions, such as inhibitors of tyrosine kinases and their receptors, drugs that interfere mitotic or target on microtubule (red box in **Fig. 3d)**.

## Performance of level two model

Performance of the DComboNet level two model was first evaluated using hepatocellular carcinoma cell line HepG2 and breast adenocarcinoma cell line MCF7. Take HepG2 as an example, gene expression profiles between HEPG2 and other cancer cell lines were compared to obtain specifically expressed genes in HepG2; gene expression profiles of HepG2 before and after monotherapy were compared to generate the differentially expressed genes (DEGs). HepG2 specific network was constructed by added 632 HepG2 specifically expressed genes, 78913 drug-DEG, 1652 drug-DEpathway associations and the corresponding gene-gene, gene-drug and gene-pathway associations. Potential drug combinations were predicted by level two model based on HepG2 specific network. The AUC of DComboNet level two model was 0.844 for HepG2, rising significantly compared with AUC of level one model (AUC = 0.787, **Fig. 4a**). The prediction on breast cancer cell lines MCF7 was also improved with the AUC rose from 0.764 to 0.795 (**Fig. 4b**).

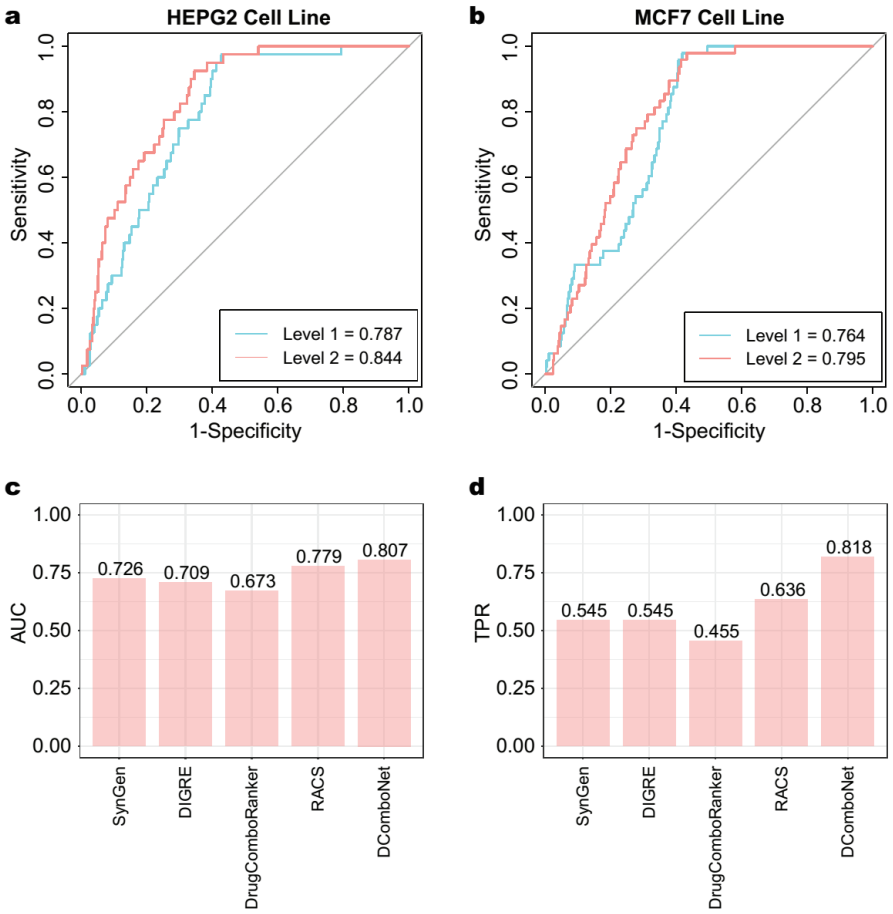


**Figure 4**. Performance of cancer sample specific drug combination prediction model. **a)** and **b)** ROC curves of model on hepatocellular carcinoma cell line, HEPG2, and breast cancer cell line, MCF7. In each plot, red and blue curves indicate the ROC curves of level two model and level one model, and the number in legend indicate the AUC values. **c-d)** Method comparison between DComboNet level two model and other prediction algorithms (SynGen, DIGRE, DrugComboRanker, RACS) using the OCI-LY3 dataset.

Some drug combinations, especially standard chemotherapy that directly act on DNA/RNA, cannot be correctly predicted in the level one model. By adding drug perturbated transcriptome change, the effects of these drugs on cancer cells can be reflected through changes in a series of genes or pathways instead of only their target genes, therefore correct prediction may be obtained. For example, the combination of capecitabine and docetaxel are both standard chemotherapies with a broad anti-cancer effect[21]. Although they show relatively high pharmacological drug similarity ( $sim_{DD}(\text{capecitabine}, \text{docetaxel}) = 0.695$ ), the target genes and the biological functions between capecitabine and docetaxel are distinctive (target distance is 2, pathway similarity is 0.45)

[22, 23]. This combination failed at predicting as combinable pair in level one model, but was successfully predicted in level two model after reconstructing cancer sample specific network.

We further compared DComboNet level two model and other four drug combination prediction algorithms (SynGen[9], DIGRE[10], DrugComboRanker [19], and RACS[11]) which also used the change of transcriptome profiles before and after monotherapy treatments. All of these algorithms were evaluated using the drug synergy screening dataset (OCI-LY3). The overall performance of DComboNet outperformed other algorithms, especially more powerful when predicting the combinable pairs (**Fig 4c-d**). DComboNet achieves 0.807 AUC and 81.8% true positive rate. Among 11 real synergy pairs, 9 pairs were successfully predicted by DComboNet while 7, 6, 6 and 5 pairs were successfully predicted by RACS, SynGen, DIGRE and DrugComboRanker, respectively (**Fig 4d**).

# Case study: HepG2 - sorafenib

Hepatocellular carcinoma (HCC) is the fourth leading cause of cancer death with only few approved agents as first line treatment, such as sorafenib[24-26]. However, most patients will develop sorafenib resistance eventually which include multiple biological pathways. Therefore, it is critical to find potential drug combination to improve the efficacy of single sorafenib treatment. We predicted combinable drugs for sorafenib treatment through DComboNet level two model and validated the predictions through literature investigation and in-vitro experiments. Using 'Sorafenib' as the drug seed, 5 out of 6 known combinations were predicted correctly. In the rest 26 newly predicted combinable drug pairs, 16 of them have been reported to be synergistic either in HCC models (8 pairs) or in other cancers (8 pairs) in previous literatures (**Fig.5a**).

In addition to predicting the propensity of drug combinations, DComboNet can also rank genes and pathways in the network according to the proximity relative to drug seed. Thus, analyzing the overall results may be helpful in inferring the possible mechanism of drug combinations. Among the drugs predicted as combinable candidates for sorafenib, we found three potential mechanism modes for effective combination (**Fig 5b-d**).

The first mechanism is that two drugs shared same target genes (**Fig.5b**). Among the prediction results, several multiple tyrosine kinase inhibitors (TKIs) show strong tendency to be combined with sorafenib. Imatinib, cediranib, dasatinib, sunitinib and pazopanib shared 6 targets (FLT1, FLT3, FLT4, KDR, KIT, PDGFRB) with sorafenib (Fig.5b). The combination between TKIs and sorafenib may work on cancer-related genes or functions through compensatory way to avoid single TKI resistance and further improve efficacy on cancer patients[27, 28]. For example, sorafenib can block the function of genes related to imatinib resistance in HCC treatment [29].

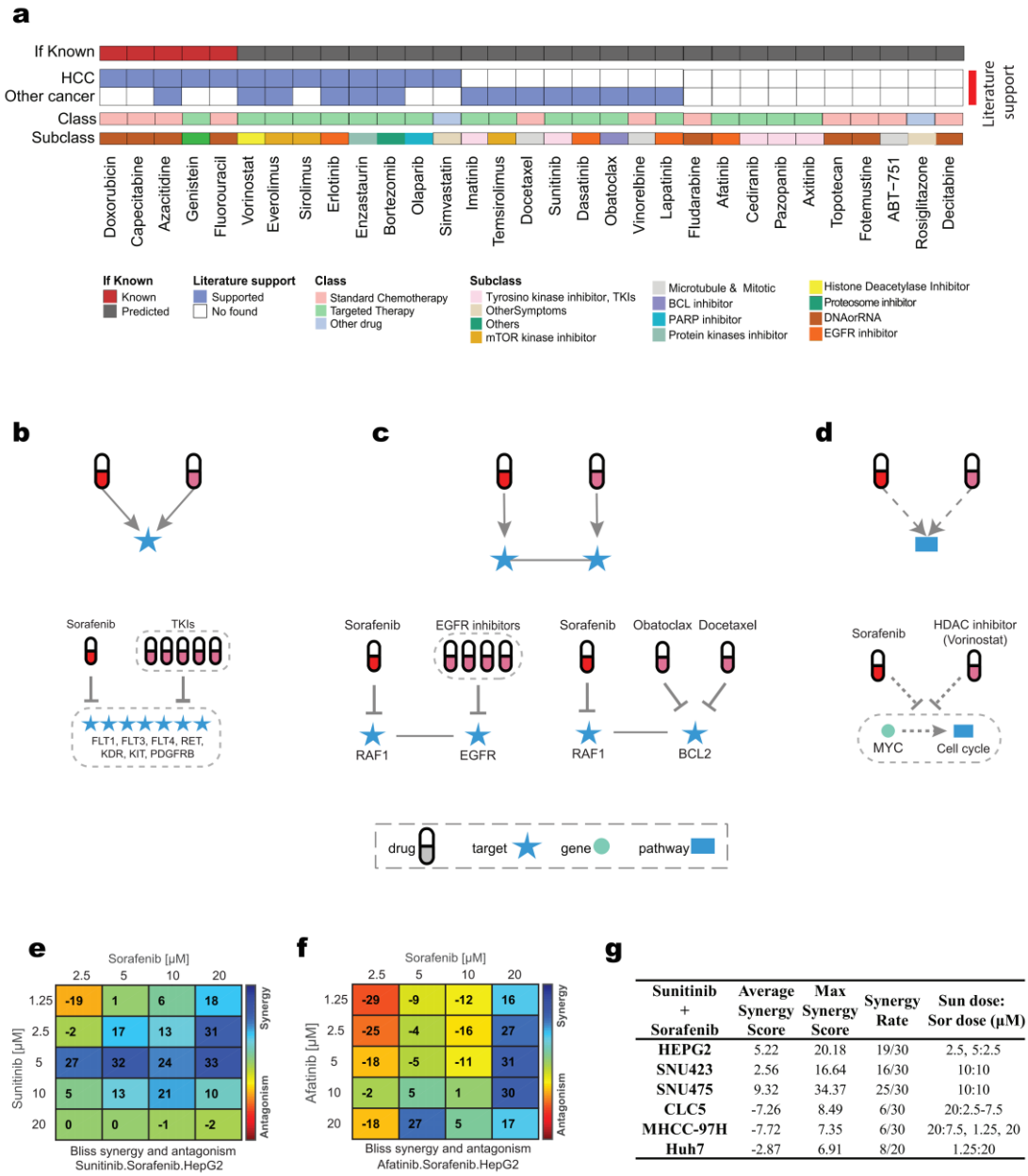


g

| Sunitinib + Sorafenib | Average Synergy Score | Max Synergy Score | Synergy Rate | Sun dose: Sor dose (μM) |
|---|---|---|---|---|
| **HEPG2** | 5.22 | 20.18 | 19/30 | 2.5, 5:2.5 |
| **SNU423** | 2.56 | 16.64 | 16/30 | 10:10 |
| **SNU475** | 9.32 | 34.37 | 25/30 | 10:10 |
| **CLC5** | -7.26 | 8.49 | 6/30 | 20:2.5-7.5 |
| **MHCC-97H** | -7.72 | 7.35 | 6/30 | 20:7.5, 1.25, 20 |
| **Huh7** | -2.87 | 6.91 | 8/20 | 1.25:20 |

**Figure 5**. Predictions and validation for Sorafenib on Hepatocellular carcinoma cell line, HEPG2 and the hypothetical mechanisms inferred. **a)** Overall prediction results for Sorafenib on HEPG2 cell line. The first line denotes if the predicted combinable drugs belong to known drug combination for Hepatocellular carcinoma (HCC); the second and third lines denote if predictions have literature supports for HCC or other cancer types; the fourth and fifth lines show the classification information of predicted drugs. **b-d)** indicate schematic diagrams of three potential combination mechanism modes for sorafenib case study. The upper part of **b)** shows the schematic diagram for drugs targeting on the same genes to achieve synergy, and the bottom shows the example "sorafenib-other tyrosine kinase inhibitors (TKIs)" matching this mode. The upper part of **c)** shows the mode that the interaction between drugs' target genes lead to synergy, and the bottom part shows two examples (sorafenib and EGFR inhibitor and sorafenib and BCL2 inhibitor). The upper part of **d** shows the synergy may through the regulation of cancer-related genes other than target genes, and the matching examples (Sorafenib and HDAC inhibitors). In figure **b-d)**, the capsule shape nodes represent drugs, dark red corresponds to sorafenib, and light red corresponds to the predicted combinable drugs; blue stars represents target genes of drug; green round dots represents other genes in gene network;

and blue rectangles represent pathways. **e-f)** Experimental validation results for sorafenib combined with sunitinib and afatinib, respectively. Each of the heatmaps shows the synergy score calculated by the Bliss method for each dose points. The color bar of heatmap shows the score range from synergy (blue) to antagonism (red). **g)** The summary table of experimental synergy screening for sorafenib and sunitinib in six hepatocellular carcinoma cell lines (HEPG2, SNU475, SNU472, Huh-7, CLC5 and MHCC-97H) with multiple dose combinations.

The second mechanism is that two drugs may achieve synergy through the regulatory relationships between their target genes (**Fig.5c**). Three epidermal growth factor receptor (EGFR) inhibitors, erlotinib, afatinib and lapatinib[22, 30] were predicted as candidates with combination potential with sorafenib. DComboNet showed that EGFR inhibitors connect to sorafenib through the 'EGFR-RAF1' link **(Fig.5c).** EGFR is an upstream signal receptor Ras pathway while RAF1 acts as a signal transduction mediate with RAS/RAF/MEK/ERK signaling pathway [31, 32]. Inhibiting EGFR can help sensitize the efficacy of RAF inhibitor (e.g. sorafenib) in hepatocellular cancer cell lines [33] and the synergism between RAF inhibitor sorafenib and EGFR inhibitors have also been observed in multiple cancer types [34-36]. Another example is the predicted combination of BCL2 inhibitor (docetaxel and obatoclax) and sorafenib**.** BCL2 inhibitor is connected with sorafenib via the association of their target genes "BCL2-RAF1" in the network **(Fig.5c)**. Over-expression of BCL2 and RAF1 may lead to sorafenib resistance, which can be altered by inhibiting BCL2 in HCC cell lines [37, 38]. This indicates that coadministration of BCL inhibitor and sorafenib may improve treatment efficacy.

The third mechanism of drugs combination is that they co-regulate cancer-related genes, even there are no direct target gene associations involved **(Fig.5d).** Take histone deacetylase (HDACs) inhibitors vorinostat as an example (**Fig.5d**). Vorinostat itself plays an important anti-cancer role which inhibit cancer cell growth via blocking cell cycle [39]. In the potential mechanism network, we found sorafenib and vorinostat are linked together via down-regulating MYC (**Fig.5d**). HDACi

has been reported to help acetylate c-MYC and promote apoptosis in AML [40]. The sorafenib-vorinostat combination may coregulate multiple pathways related to cancer cell cycle and apoptosis to achieve synergism [41].

Based on these drug combination mechanisms, we selected two drugs (sunitinib and afatinib) to further verify the predicted combination with sorafenib in HCC. Sunitinib shared 7 target genes with sorafenib (**Fig.5b**), and their combination showed synergistic efficacy in renal cell carcinoma [42]. However, there are no similar studies in HCC. Therefore, we performed the combination experiments of sorafenib and sunitinib using HCC cell line HepG2. 14 of the 20 dose combinations showed synergy, and the most synergistic dose combination was when sunitinib was 5 μM and sorafenib was 20 μM (**Fig.5e)**. Furthermore, we verified a completely new prediction result, the combination of sorafenib and afatinib. Afatinib is an EGFR inhibitor, which may achieve synergy with sorafenib through the regulatory relationships between their target genes (**Fig.5c**). Experiments in HepG2 showed 9 synergistic points at different dose, indicating that sorafenib and afatinib is combinable (**Fig.5f**).

Additionally, the combination of sorafenib and sunitinib was further tested using another five HCC cell lines (**Fig.5g)**. SNU475 and SNU432 also showed synergy in experimental screening especially strong synergy at multiple doses, while synergistic effect on Huh7, CLC5 and MHCC-97H cell lines only occurred in few dose points. This reflects the heterogeneous response of cancer cell lines to the same treatment. It is necessary to make individualized drug combination prediction. If the expression profile of individual cancer sample is available, the DComboNet level two model could obtain personalized prediction results by utilizing sample specific network.

# Discussion

Discover efficient drug combination under the highly complex and heterogeneous cancer system is difficult and time-consuming on wet-lab synergistic drug screening whereas in-silico drug combination prediction has become a critical approach in preclinical research. Based on the comprehension of anti-cancer drug mechanism and the accumulation of cancer related data, we developed a two-level prediction model DComboNet. Level one model can be used to predict anti-cancer drug combination in a more general manner, whereas level two model is capable to achieve cancer sample specific drug combination prediction by integrating sample specific expressed genes, differentially expressed genes and biological pathways after drug treatment into the 'drug-gene/pathway' network.

DComboNet has several advantages: 1) DComboNet utilizes the complex multi-layer heterogeneous networks, which efficiently integrate multi-level data and provide more information to rank the combinable tendency from a holistic point of view. Therefore, DComboNet is possible to predict drug pairs that have a more intricate combination mechanisms other than the direct target gene association. 2) DComboNet contains two levels of models, which users can choose according to their aim and available data. Level two model has better prediction accuracy than level one, but requires the expression profiles of cancer sample before and after monotherapy treatment. 3) Compared to other algorithms using similar input data, DComboNet achieves higher true positive rate. 4) DComboNet provides drug-gene/pathway network between the predicted combinable drug pairs, which is helpful for understanding the potential mechanism of drug synergy.

We noted that certain drug combinations are usually poorly predicted, especially those with lower

pharmacological similarities and less functionally relationship in gene or pathway network. Additionally, DComboNet ranks candidate drugs based on their global similarity with the seed drug, therefore it may have less power on predicting drug combinations with distinct mechanisms. With the accumulation of high-throughput drug screening data, we plan to combine DComboNet with supervised machine learning algorithms to improve the prediction performance. We also realized that the different response between cancer cell lines and patients under the same drug treatment still remains as a common obstacle for drug discovery transformation. Drug absorption, distribution, metabolism and excretion process cannot be well modelled under the context of cancer cell lines. Patient-derived mouse xenograft may serve as a better model than cell line for these, but drug screening on animal model like mouse need more effort and funding. Although there are many difficulties in the translation from basic research to application, computational prediction of drug combinations is fast and convenient as well as achieves much better accuracy than random. We anticipate that DComboNet could provide candidates for drug combination experiments and accelerate the discovery of new synergistic drugs.

# Methods

## Data collection

Known drug combinations were collected from DCDB 2.0 [43]. Only FDA approved drugs or drugs entering phase III or IV of clinical trial were kept in the subsequent analysis. Therapeutic information used to construct drug-drug association network included: drug ATC (Anatomical Therapeutic Chemical Classification System) codes[44] extracted from WHO Collaborating Centre for Drug Statistics Methodology (WHOCC) website, chemical structures downloaded from

DrugBank[22, 45] and PubChem[46], drug side effect information collected from SIDER4[47]. Drug target proteins or genes were retrieved from Drugbank and Therapeutic Target Database (TTD)[48]; Drug related genes were obtained from IPA (Ingenuity® Pathway Analysis).

The human protein-protein interaction network were extracted from the scored InBio Map [49]. The interaction pairs with low score (score < 0.15) were removed. Cancer related genes were extracted from KEGG Cancer related pathways [50].

Gene expression profiles of drug perturbated cancer cell lines were downloaded from LINCS database[8] and DREAM challenge 2014[9]. LINCS database provided gene expression microarray data for 1127 cell lines treated by 41847 molecules. Drug treated hepatocellular carcinoma cell line HepG2 and breast cancer cell line MCF7 were extracted from LINCS. The pretreated gene expression data of HepG2 and MCF7 were downloaded from CCLE database[6].

## Level one model: Cancer Drug Combination Network (DComboNet)

Cancer Drug Combination Network (DComboNet) is based on a multi-level heterogenous network which contains five subnetworks, drug-drug association network ($N_{DD}$), drug-gene association network ($N_{DG}$) and gene-gene association network ($N_{GG}$), drug-pathway association network ($N_{DP}$) and pathway-pathway association network ($N_{PP}$). The details of subnetwork construction are described in Supplement methods. Briefly speaking, $N_{DD}$ obtained drugs from known drug combinations and their associations was weighted by pharmacological similarity integrated three kinds of drug similarity. For level one model, $N_{DG}$ was constructed based on drug and target (D-T) associations, drug and drug-related gene (D-G) associations. $N_{GG}$ integrated both cancers related genes extracted from KEGG cancer related pathway including 'pathway in cancer'

and genes connected with drugs in $N_{DG}$, and the associations between genes were extracted from inBio Map (V 2016_09_12) [49]. $N_{DP}$ was constructed based on the association between drugs and their possible regulated pathways. $N_{PP}$ was built on the hierarchy of KEGG provided in WNS method [18].

The network can be represented as an adjacency matrix $A = \begin{bmatrix} A_{DD} & A_{DG} & A_{DP} \\ A_{GD} & A_{GG} & A_{PG} \\ A_{PD} & A_{GP} & A_{PP} \end{bmatrix}$, where $A_{GD}$ and $A_{PD}$ are transpose of $A_{DG}$ and $A_{DP}$. Given a certain drug, DComboNet recommends drugs with closest topological relationship as the combinable candidates. This global proximity between drugs can be captured via random walking with restart (RWR) algorithm. This algorithm originally designed to simulate a random walker walking on the network with certain initial probability corresponding network. For our task, we assigned the walk starts only from $N_{DD}$. More specific, the random walker is assigned as a drug seed with an initial probability $P_0 = \begin{Bmatrix} [1\ 0 \dots 0]_M^T \\ [0 \dots 0]_N^T \\ [0 \dots 0]_L^T \end{Bmatrix}$, where M, N and L indicate the node number in $N_{DD}$, $N_{GG}$ and $N_{PP}$, respectively. Walker will start from this drug seed node to traverse every node in network. At every step, the jumping happens from the current node to it direct neighbor(s) with a probability $1 - \sigma$ or returns to the drug node with a restart probability $\sigma$. The probability in $t + 1$ step can be represented as follow:

$$P_{t+1} = (1 - \sigma)HP_t + \sigma P_0 \quad (1)$$

After several iterations, the probability will reach a steady state when the difference between $P_{t+1}$ and $P_t$ falls below $10^{-10}$. At this point, all nodes in the complex network have obtained global proximity relative to the drug seed which can be considered as the combination potential. After removing the known drug combinations, the rest candidate drugs can be ranked according to their potential.

In function (1), $\mathrm{H} = \begin{bmatrix} H_{DD} & H_{DG} & H_{DP} \\ H_{GD} & H_{GG} & O_{PG} \\ H_{PD} & O_{GP} & H_{PP} \end{bmatrix}$ denotes the transition matrix which reflects different strategies for the walker to traverse the complex network.

The transition probability between drug 1 ($d1$) and drug 2 ($d2$) can then be described as:

$$H_{DD}(d1,\ d2) = \begin{cases} \dfrac{A_{DD}(d1,d2)}{\sum_{d=1}^{M} A_{DD}(d1,\ d)} & ,if\ \sum_{g=1}^{N} E_{DG}(d1\ or\ d2,\ g) = 0\ and\ \sum_{p=1}^{L} E_{DP}(d1\ or\ d2,\ p) = 0 \\ \dfrac{\lambda_D A_{DD}(d1,d2)}{\sum_{d=1}^{M} A_{DD}(d1,\ d)} & ,others \end{cases} \quad (2)$$

The jumping within drug network contains two different possibilities: if drug does not have any link with $\mathrm{N_{GG}}$ or $\mathrm{N_{PP}}$, the jump happens in $\mathrm{N_{DD}}$ with probability $\lambda_{\mathrm{D}} = 1$; if $d1$ or $d2$ can be linked to any gene node ($g$) and/or pathway node ($p$), the potential jumping happens within $\mathrm{N_{DD}}$ with the probability $\lambda_{\mathrm{D}}$.

If drug can be linked to $\mathrm{N_{GG}}$, jumping from $d1$ to gene 1 ($g1$) may happen with the probability $\lambda_{\mathrm{DG}}$ and the transition probability can be described as:

$$H_{DG}(d1,\ g1) = \begin{cases} \dfrac{\lambda_{DG} A_{DG}(d1,g1)}{\sum_{\mathrm{g}=1}^{N} E_{DG}(d1,g)} & ,if\ \sum_{g=1}^{N} E_{DG}(d1,\ \mathrm{g}) \neq 0 \\ 0 & ,others \end{cases} \quad (3)$$

After the jumping fall in $\mathrm{N_{GG}}$, the transition probability from gene $g1$ to gene $g2$ in $\mathrm{N_{GG}}$ can be influenced by the existence of edges in $\mathrm{N_{GD}}$. Therefore, the transition probability within $\mathrm{N_{GG}}$ can be computed as:

$$H_{GG}(g1,\ g2) = \begin{cases} \dfrac{A_{GG}(g1,g2)}{\sum_{g=1}^{N} A_{GG}(g1,\ g)} & ,if\ \sum_{d=1}^{M} E_{DG}(g1\ or\ g2,\ \mathrm{d}) = 0\ and\ \sum_{p=1}^{L} E_{GP}(g1\ or\ g2,\ p) = 0 \\ \dfrac{\lambda_G A_{GG}(g1,g2)}{\sum_{g=1}^{N} A_{GG}(g1,\ g)} & ,others \end{cases} \quad (4)$$

Similarly, if jump happens from $\mathrm{N_{GG}}$ back to $\mathrm{N_{DD}}$, transition probability between $g2$ and $d2$ can be described as:

$$H_{GD}(g2,\ d2) = \begin{cases} \frac{\lambda_{DG} A_{DG}(g2, d2)}{\sum_{d=1}^{M} E_{DG}(g2,\ d)} & ,if \sum_{d=1}^{M} E_{DG}(g2, d) \neq 0 \\ 0 & ,\ others \end{cases} \quad (5)$$

Similar to the jumping strategy through gene node, transition probability between $d1$ and pathway node $p1$ can be calculated as:

$$H_{DP}(d1,\ p1) = \begin{cases} \frac{\lambda_{DP} A_{DP}(d1, \mathrm{p1})}{\sum_{p=1}^{L} E_{DP}(d1, p)} & ,if \sum_{p=1}^{L} E_{DP}(d1,\ p) \neq 0 \\ 0 & ,\ others \end{cases} \quad (6)$$

When the jump falls in $\mathrm{N_{PP}}$, we expected the next step can directly happen from $\mathrm{N_{PP}}$ back to $\mathrm{N_{DD}}$. More specific, if the edge(s) between drug and pathway exist, jump can only happen either within $\mathrm{N_{PP}}$ or between $\mathrm{N_{DP}}$. The calculation of transition probability within $\mathrm{N_{PP}}$ can be seen as follow:

$$H_{PP}(p1, p2) = \begin{cases} \frac{A_{PP}(p1, p2)}{\sum_{p=1}^{L} A_{PP}(p1,\ p)} & ,if \sum_{d=1}^{M} E_{DP}(p1\ or\ p2,\ d) = 0 \\ \frac{\lambda_P A_{PP}(p1, p2)}{\sum_{\mathrm{p}=1}^{l} A_{PP}(p1,\ p)} & ,\ others \end{cases} \quad (7)$$

The jump from $\mathrm{p2}$ back to $\mathrm{d2}$ can then be described as:

$$H_{PD}(p2,\ d2) = \begin{cases} \frac{\lambda_{DP} A_{DP}(p2, d2)}{\sum_{d=1}^{M} E_{DP}(p2,\ d)} & ,if \sum_{d=1}^{M} E_{DP}(p2, d) \neq 0 \\ 0 & ,\ others \end{cases} \quad (8)$$

From the description of jumping strategy between $\mathrm{d1}$ and $\mathrm{d2}$, we can see that jumping probability $\lambda$ are not independent. Within the homological subnetworks, $\lambda$s are equal ($\lambda_D = \lambda_G = \lambda_P$). The jumping probability in heterogenous subnetwork (such as $\mathrm{N_{DG}}$ and $\mathrm{N_{DP}}$) are influenced by those within homological subnetworks ($\lambda_{DG} = 1 - \lambda_D$ and $\lambda_{DP} = 1 - \lambda_D$).

To improve the accuracy of the model, global restart probability $\sigma$ and jumping probabilities ($\lambda_{\mathrm{D}}$) were set to values from 0 to 1 and the optimal parameters were selected through cross-validation (supplement figure 1). Based on the tuning results, the default setting of $\lambda_{\mathrm{D}}$ is set as 0.5 to keep the balanced contribution of sub-networks, and $\sigma$ is set as 0.7 which is also consistence with previous publications [51].

## Level two model: cancer-specific DComboNet

To predict sample specific drug combination, transcriptome data before and after drug perturbation were further integrated in the $N_{DG}$ and $N_{GG}$ as well as $N_{DP}$ and $N_{PP}$ to construct sample specific complex network.

The specifically expressed genes ($G_{cancer}$) were selected with the criteria $\left|Expr_j - \frac{\sum_{j=1}^{j=k} Expr_j}{k}\right| > 1.5$ (that the fold change of gene expression between the specific cancer cell line and the average of expression value of all the other cell lines above 1.5). $G_{cancer}$ were used to replace the nodes in $N_{GG}$ for reconstruct cancer-specific gene-gene association network.

Cancer specific drug-gene and drug-pathway associations were added into the original drug-gene/pathway association network $N_{DG}$ and $N_{DP}$. These two associations were obtained by comparing drug treated gene expression data and DMSO. Differentially expressed genes were selected by functions lmFIt and eBayes in the Limma package ($FDR < 0.1$) [52]. Differential regulated pathways (DEpathway) were obtained by the GSVA algorithm (FDR <0.1) [53]. The edge weight of both drug-DEG were assigned as the fold changes of genes perturbated by drugs and drug-DEpathway were assigned as 1. Furthermore, these differentially expressed genes and their protein-protein interactions extracted from InBio Map were also added into $N_{GG}$.

Similar to Level two model, a given drug was set to be the seed with initial probability $P_0$ and iterated till the steady status of the probability of nodes. Then the candidate drugs will be ranked based on the final probability after removing the drug pairs in positive set.

### Cross validation and independent test

We conducted Leave-One-Drug-pair-Out Cross Validation (LODOCV) to assess the model

469 performance. For each known drug combination, the edge weight was replaced by its integrated
470 pharmacological similarity score and every drug in the combination will be used as drug seed to
471 rank the rest of drugs in the network. Receiver operating characteristic (ROC) curves and the area
472 under these curves (AUC) were also used to quantify the performance. To access the successfully
473 predicted drug pairs and avoid the asymmetrical ranks, that is, the difference between the rank of B
474 when A is used as drug seed and the rank of A when B is taken as seed, a two-threshold strategy was
475 used to classify the drug pair into combinable, uncombinable and intermediate (Supplementary
476 method).

477 To further verify the predictability and generalization of our level two model in independent
478 dataset, we tested the model performance using the OCI-LY3 dataset [9]. Excess over Bliss (E.o.B.)
479 and signal to noise ratio (s.n.r.) were calculated by the Bliss independent model [9]. Drug pairs were
480 classified into combinable pairs (synergistic, E.o.B.>0 and s.n.r.>2) and uncombinable pairs
481 (antagonistic and additive).

482 **Experimental validation**

483 Potential combinations between sorafenib and sunitinib, sorafenib and afatinib were evaluated
484 using liver cancer cell lines (Supplementary method). Cell viability matrices of each drug pair on
485 the corresponding cell lines were used as the input data to calculate experimental synergy score with
486 Bliss model provided by Combenefit software [54]. To reflect the degree of synergy, the maximum
487 synergy score (Max Syn) and the synergy rate among all dose combinations was calculated.
488

**Code availability**

DComboNet is implemented in R language and available at https://github.com/VeronicaFung/DComboNet .

# ACKNOWLEDGEMENTS

This work was supported by the National Natural Science Foundation of China 31771472), National Key Research and Development Project (2019YFC1315804), Chinese Academy of Sciences (ZDBS-SSW-DQC-02), SA-SIBS Scholarship Program, Shanghai Municipal Science and Technology Major Project (No.2018SHZDZX01), LCNBI and ZJLab.

# AUTHOR CONTRIBUTIONS

F.Y.M.F. and H.L. designed the study; F.Y.M.F. performed model construction and data analysis; Z.T.Z. performed drug combination screening experiments; F.Y.M.F. wrote the manuscript; F.Y.M.F. developed the R package; Y.X.L. and H.L. supervised research and revised the manuscript.

# DISCLOSURE DECLARATION

The authors declare that they have no competing interests.

# Reference

1. Bray, F., et al., *Global cancer statistics 2018: GLOBOCAN estimates of incidence and mortality worldwide for 36 cancers in 185 countries.* CA Cancer J Clin, 2018. **68**(6): p. 394-424.
2. Al-Lazikani, B., U. Banerji, and P. Workman, *Combinatorial drug therapy for cancer in the post-genomic era.* Nat Biotechnol, 2012. **30**(7): p. 679-92.
3. Sun, X., S. Vilar, and N.P. Tatonetti, *High-throughput methods for combinatorial drug discovery.* Sci Transl Med, 2013. **5**(205): p. 205rv1.
4. He, L., et al., *Methods for high-throughput drug combination screening and synergy scoring*, in *Cancer systems biology*. 2018, Springer. p. 351-398.

5. Zhao, X.M., et al., *Prediction of drug combinations by integrating molecular and pharmacological data.* PLoS Comput Biol, 2011. **7**(12): p. e1002323.
6. Barretina, J., et al., *The Cancer Cell Line Encyclopedia enables predictive modelling of anticancer drug sensitivity.* Nature, 2012. **483**(7391): p. 603-7.
7. Ghandi, M., et al., *Next-generation characterization of the Cancer Cell Line Encyclopedia.* Nature, 2019. **569**(7757): p. 503-508.
8. Subramanian, A., et al., *A Next Generation Connectivity Map: L1000 Platform and the First 1,000,000 Profiles.* Cell, 2017. **171**(6): p. 1437-1452 e17.
9. Bansal, M., et al., *A community computational challenge to predict the activity of pairs of compounds.* Nat Biotechnol, 2014. **32**(12): p. 1213-22.
10. Yang, J., et al., *DIGRE: Drug-Induced Genomic Residual Effect Model for Successful Prediction of Multidrug Effects.* 2015. **4**(2): p. 91-97.
11. Sun, Y., et al., *Combining genomic and network characteristics for extended capability in predicting synergistic drugs for cancer.* Nat Commun, 2015. **6**(1): p. 8481.
12. O'Neil, J., et al., *An Unbiased Oncology Compound Screen to Identify Novel Combination Strategies.* Mol Cancer Ther, 2016. **15**(6): p. 1155-62.
13. Menden, M.P., et al., *Community assessment to advance computational prediction of cancer drug combinations in a pharmacogenomic screen.* Nat Commun, 2019. **10**(1): p. 2674.
14. Preuer, K., et al., *DeepSynergy: predicting anti-cancer drug synergy with Deep Learning.* Bioinformatics, 2018. **34**(9): p. 1538-1546.
15. Chen, D., et al., *Systematic synergy modeling: understanding drug synergy from a systems biology perspective.* BMC Syst Biol, 2015. **9**(1): p. 56.
16. Dorel, M., et al., *Network-based approaches for drug response prediction and targeted therapy development in cancer.* Biochem Biophys Res Commun, 2015. **464**(2): p. 386-91.
17. Huang, J.L., et al., *Systematic Prediction of Pharmacodynamic Drug-Drug Interactions through Protein-Protein-Interaction Network.* Plos Computational Biology, 2013. **9**(3).
18. Chen, D., et al., *Synergy evaluation by a pathway–pathway interaction network: a new way to predict drug combination.* 2016. **12**(2): p. 614-623.
19. Huang, L., et al., *DrugComboRanker: drug combination discovery based on target network analysis.* Bioinformatics, 2014. **30**(12): p. i228-36.
20. Cheng, F., I.A. Kovács, and A.-L.J.N.c. Barabási, *Network-based prediction of drug combinations.* 2019. **10**(1): p. 1-11.
21. Mandelblat, J., T. Bashir, and D.R.J.E.r.o.a.t. Budman, *Capecitabine–docetaxel combination treatment.* 2006. **6**(9): p. 1169-1178.
22. Wishart, D.S., et al., *DrugBank: a knowledgebase for drugs, drug actions and drug targets.* Nucleic Acids Res, 2008. **36**(Database issue): p. D901-6.
23. Gligorov, J. and J.P. Lotz, *Preclinical pharmacology of the taxanes: implications of the differences.* Oncologist, 2004. **9 Suppl 2**: p. 3-8.
24. Llovet, J.M., et al., *Sorafenib in advanced hepatocellular carcinoma.* N Engl J Med, 2008. **359**(4): p. 378-90.
25. Kulik, L. and H.B. El-Serag, *Epidemiology and Management of Hepatocellular Carcinoma.* Gastroenterology, 2019. **156**(2): p. 477-491 e1.
26. El-Serag, H.B.J.T.L.B. and Pathobiology, *Epidemiology of hepatocellular carcinoma.* 2020:

p. 758-772.

27. Haas, N.B., et al., *Adjuvant sunitinib or sorafenib for high-risk, non-metastatic renal-cell carcinoma (ECOG-ACRIN E2805): a double-blind, placebo-controlled, randomised, phase 3 trial.* Lancet, 2016. **387**(10032): p. 2008-16.

28. Buchler, T., et al., *Sunitinib followed by sorafenib or vice versa for metastatic renal cell carcinoma--data from the Czech registry.* Ann Oncol, 2012. **23**(2): p. 395-401.

29. Guo, T., et al., *Sorafenib inhibits the imatinib-resistant KITT670I gatekeeper mutation in gastrointestinal stromal tumor.* 2007. **13**(16): p. 4874-4881.

30. Xia, W., et al., *Anti-tumor activity of GW572016: a dual tyrosine kinase inhibitor blocks EGF activation of EGFR/erbB2 and downstream Erk1/2 and AKT pathways.* Oncogene, 2002. **21**(41): p. 6255-63.

31. Ezzoukhry, Z., et al., *EGFR activation is a potential determinant of primary resistance of hepatocellular carcinoma cells to sorafenib.* 2012. **131**(12): p. 2961-2969.

32. Huether, A., et al., *EGFR blockade by cetuximab alone or as combination therapy for growth control of hepatocellular cancer.* 2005. **70**(11): p. 1568-1578.

33. Ezzoukhry, Z., et al., *EGFR activation is a potential determinant of primary resistance of hepatocellular carcinoma cells to sorafenib.* Int J Cancer, 2012. **131**(12): p. 2961-9.

34. Blivet-Van Eggelpoël, M.-J., et al., *Epidermal growth factor receptor and HER-3 restrict cell response to sorafenib in hepatocellular carcinoma cells.* 2012. **57**(1): p. 108-115.

35. Duran, I., et al., *Phase I targeted combination trial of sorafenib and erlotinib in patients with advanced solid tumors.* Clin Cancer Res, 2007. **13**(16): p. 4849-57.

36. Martinelli, E., et al., *Synergistic antitumor activity of sorafenib in combination with epidermal growth factor receptor inhibitors in colorectal and lung cancer cells.* Clin Cancer Res, 2010. **16**(20): p. 4990-5001.

37. Yang, F., et al., *MicroRNA-34a targets Bcl-2 and sensitizes human hepatocellular carcinoma cells to sorafenib treatment.* Technol Cancer Res Treat, 2014. **13**(1): p. 77-86.

38. Tutusaus, A., et al., *Antiapoptotic BCL-2 proteins determine sorafenib/regorafenib resistance and BH3-mimetic efficacy in hepatocellular carcinoma.* Oncotarget, 2018. **9**(24): p. 16701-16717.

39. Grant, S., C. Easley, and P. Kirkpatrick, *Vorinostat*. 2007, Nature Publishing Group.

40. Nebbioso, A., et al., *c-Myc modulation and acetylation is a key HDAC inhibitor target in cancer.* 2017. **23**(10): p. 2542-2555.

41. Yuan, H., et al., *Inhibition of autophagy significantly enhances combination therapy with sorafenib and HDAC inhibitors for human hepatoma cells.* 2014. **20**(17): p. 4953.

42. Dudek, A.Z., et al., *Sequential therapy with sorafenib and sunitinib in renal cell carcinoma.* Cancer, 2009. **115**(1): p. 61-7.

43. Liu, Y., et al., *DCDB 2.0: a major update of the drug combination database.* Database (Oxford), 2014. **2014**: p. bau124.

44. Miller, G.C. and H. Britt, *A new drug classification for computer systems: the ATC extension code.* Int J Biomed Comput, 1995. **40**(2): p. 121-4.

45. Wishart, D.S., et al., *DrugBank: a comprehensive resource for in silico drug discovery and exploration.* Nucleic Acids Res, 2006. **34**(Database issue): p. D668-72.

46. Kim, S., et al., *PubChem 2019 update: improved access to chemical data.* Nucleic Acids Res, 2019. **47**(D1): p. D1102-D1109.

603 47. Kuhn, M., et al., *The SIDER database of drugs and side effects.* Nucleic Acids Res, 2016.
604 **44**(D1): p. D1075-9.
605 48. Wang, Y., et al., *Therapeutic target database 2020: enriched resource for facilitating*
606 *research and early development of targeted therapeutics.* Nucleic Acids Res, 2020. **48**(D1):
607 p. D1031-D1041.
608 49. Li, T., et al., *A scored human protein–protein interaction network to catalyze genomic*
609 *interpretation.* 2017. **14**(1): p. 61.
610 50. Kanehisa, M. and S.J.N.a.r. Goto, *KEGG: kyoto encyclopedia of genes and genomes.* 2000.
611 **28**(1): p. 27-30.
612 51. Valdeolivas, A., et al., *Random walk with restart on multiplex and heterogeneous biological*
613 *networks.* Bioinformatics, 2019. **35**(3): p. 497-505.
614 52. !!! INVALID CITATION !!! .
615 53. Hanzelmann, S., R. Castelo, and J. Guinney, *GSVA: gene set variation analysis for*
616 *microarray and RNA-Seq data.* Bmc Bioinformatics, 2013. **14**(1): p. 7.
617 54. Di Veroli, G.Y., et al., *Combenefit: an interactive platform for the analysis and visualization*
618 *of drug combinations.* Bioinformatics, 2016. **32**(18): p. 2866-8.
619